Genome-Wide Expression Profiling Reveals EBV-Associated Inhibition of MHC Class I Expression in Nasopharyngeal Carcinoma

Srikumar Sengupta,[1,3] Johan A. den Boon,[1,3] I-How Chen,[9] Michael A. Newton,[4,5] David B. Dahl,[6] Meng Chen,[4] Yu-Juen Cheng,[10] William H. Westra,[8] Chien-Jen Chen,[10] Allan Hildesheim,[7] Bill Sugden,[3] and Paul Ahlquist[1,2,3]

[1]Institute for Molecular Virology, [2]Howard Hughes Medical Institute, [3]McArdle Laboratory for Cancer Research, [4]Department of Statistics, and [5]Department of Biostatistics and Medical Informatics, University of Wisconsin-Madison, Madison, Wisconsin; [6]Department of Statistics, Texas A&M University, College Station, Texas; [7]Division of Cancer Epidemiology and Genetics, National Cancer Institute, Bethesda, Maryland; [8]Department of Otolaryngology-Head and Neck Surgery, The Johns Hopkins Medical Institutions, Baltimore, Maryland; and [9]MacKay Memorial Hospital and [10]National Taiwan University, Taipei, Taiwan

Abstract

To identify the molecular mechanisms by which EBV-associated epithelial cancers are maintained, we measured the expression of essentially all human genes and all latent EBV genes in a collection of 31 laser-captured, microdissected nasopharyngeal carcinoma (NPC) tissue samples and 10 normal nasopharyngeal tissues. Global gene expression profiles clearly distinguished tumors from normal healthy epithelium. Expression levels of six viral genes (*EBNA1, EBNA2, EBNA3A, EBNA3B, LMP1*, and *LMP2A*) were correlated among themselves and strongly inversely correlated with the expression of a large subset of host genes. Among the human genes whose inhibition was most strongly correlated with increased EBV gene expression were multiple MHC class I HLA genes involved in regulating immune response via antigen presentation. The association between EBV gene expression and inhibition of MHC class I HLA expression implies that antigen display is either directly inhibited by EBV, facilitating immune evasion by tumor cells, and/or that tumor cells with inhibited presentation are selected for their ability to sustain higher levels of EBV to take maximum advantage of EBV oncogene-mediated tumor-promoting actions. Our data clearly reflect such tumor promotion, showing that deregulation of key proteins involved in apoptosis (BCL2-related protein A1 and Fas apoptotic inhibitory molecule), cell cycle checkpoints (AKIP, SCYL1, and NIN), and metastasis (matrix metalloproteinase 1) is closely correlated with the levels of EBV gene expression in NPC. (Cancer Res 2006; 66(16): 7999-8006)

Introduction

Annually, 80,000 people are diagnosed with and 60,000 to 70,000 people die of nasopharyngeal carcinoma (NPC; ref. 1), with the highest incidence in Southeast Asia. Approximately 25% of cases are keratinizing squamous cell carcinomas, but ~75% are differentiated or undifferentiated nonkeratinizing carcinomas (2), invariably positive for EBV. The role of EBV in NPC and in other epithelial tumors remains poorly understood. EBV has been studied extensively in B cells, which are readily infected and usually retain EBV DNA on passaging. In contrast, EBV is strongly associated with NPC cells in tumors but easily lost from NPC cells in culture, suggesting that selective advantages that EBV provides to the tumor are not needed on explantation.

NPC incidence among Cantonese people from Guangdong is >25-fold higher than average, indicating genetic or environmental predispositions. Specific HLA types (reviewed in ref. 3 and references therein) or chromosomal regions closely linked to the HLA locus (4) are associated with increased NPC risk. High-resolution genotyping implicated the HLA-A2 subtype, prevalent among Chinese (5), but the mechanism of increased susceptibility is unknown.

Other NPC risk factors include consumption of volatile nitrosamines introduced during traditional food preparation (6) as well as polymorphisms in CYP2E1, which activates nitrosamines into reactive, DNA-damaging intermediates (7, 8), and in hOGG1 and XRCC1, involved in DNA repair (9).

To uncover mechanisms linking these complex risk factors to NPC, it is essential to study the interrelations of host and viral gene expression. Earlier studies measured human gene expression using low-density cDNA arrays and used NPC cell lines rather than tumors (10) or used bulk NPC specimens containing significant amounts of nonepithelial cells (11). A recent study addressed some of these limitations by using higher density cDNA arrays (~9,000 cDNA clones) and laser-microdissected tissue but had a limited sample size ($n = 8$) and used reference RNA from pooled cell lines, including many nonepithelial types (12). None of these studies analyzed EBV gene expression.

We describe the first comprehensive NPC gene expression study using laser capture microdissected tissue from 31 tumors and 10 normal healthy nasopharyngeal epithelium specimens, analyzed for essentially all human mRNAs and all EBV latent genes. Our results identify a panel of human genes differentially expressed in NPC versus normal healthy nasopharyngeal epithelium and reveal that EBV gene expression levels closely correlate with inhibited expression of a subset of human genes, notably genes involved in MHC class I–mediated antigen presentation.

Materials and Methods

NPC samples. Tumor and healthy nasopharyngeal tissue from areas macroscopically not involved in the tumor was collected with informed

consent from 61 Taiwanese patients. After resection, specimens were immediately flash frozen and stored in liquid nitrogen. Fifty-five cases were confirmed to be NPC and 6 as biopsy negative. Human Subjects Institutional Review Boards of National Taiwan University (Taipei, Taiwan), University of Wisconsin-Madison (Madison, WI), and U.S. National Cancer Institute (Bethesda, MD) approved this study.

Tissue processing. Frozen biopsies were embedded in Tissue-Tek OCT (Sakura Finetek, Torrance, CA) for serial 6-μm cryosectioning. Step sections were stained with H&E, and intervening unstained sections were evaluated for cytokeratins using monoclonal mouse anti-human cytokeratin antibody (AE1/AE3, 1:20 dilution) and EnVision+ System Peroxidase (3,3′-diaminobenzidine, DAKO Corp., Carpinteria, CA). EBV-harboring cells were identified by detecting EBV-encoded small RNAs (EBER) using the EBV Probe *In situ* Hybridization kit (NCL-EBV-K, Novocastra Laboratories, Newcastle upon Tyne, United Kingdom). Supplementary Table S1 lists histology results and tumor stage. Laser capture microdissection (LCM) was done on tumor samples containing <70% tumor cells and to dissect epithelial cells from normal healthy nasopharyngeal specimens using an Arcturus PixCell II LCM microscope and CapSure Macro LCM caps (Arcturus Bioscience, Mountain View, CA). For orientation, unstained sections were briefly dipped in hematoxylin, step dehydrated through increasing ethanol concentrations, and air dried. Typically, from one to a few thousand cells per sample were captured. RNA was extracted using Trizol (Invitrogen, Carlsbad, CA), DNase I treated, and amplified twice using Affymetrix Small Sample Labeling Protocol VII (Affymetrix, Santa Clara, CA) that preserves original sample mRNA representation (13). One twentieth of second-round cDNA was used to assay amplification by measuring β-actin using the QuantiTect SYBR Green Real-time PCR kit (Qiagen, Valencia, CA).

Microarray analysis. Using the BioArray High Yield RNA Labeling kit (Enzo Life Sciences, Farmingdale, NY), half of the second-round cDNA was used to synthesize biotinylated antisense RNA, which was hybridized to Affymetrix HG U133 Plus 2.0 microarrays containing 54,675 probesets for >47,000 transcripts and variants, including 38,500 human genes.[11] A typical probeset contains eleven 25-mer oligonucleotide pairs (a perfect match and a mismatch control). Some genes are measured by multiple probesets.

Quantitative real-time PCR. Using AmpliTaq Gold (Applied Biosystems, Foster City, CA) on an ABI Prism 7700, quantitative real-time PCRs contained one thirtieth of the second-round cDNA, 0.5 μmol/L of each primer, 0.2 μmol/L FAM/TAMRA-labeled probe (MWG Biotech, High Point, NC), and 1× ROX reference dye (Invitrogen). See Supplementary Table S2 for primers and probes.

Microarray data analysis. Probeset summary measures were computed by robust multiarray averaging (14) of all 41 arrays. Global gene expression was analyzed by unsupervised hierarchical clustering and multidimensional scaling. A series of statistical filters, including fold changes, *t* tests, and mixture model scores (15), identified altered gene expression. Spearman rank correlation calculations evaluated viral-host gene expression associations. Detailed description of statistical methods is in Supplementary Data.

Gene ontology and Ingenuity pathway analysis. Gene ontology analysis categorizes genes into biologically meaningful groups (16). Gene ontology annotations enriched for genes whose expression was altered between tumor and normal samples or correlated with EBV gene expression were identified using Pearson χ^2 tests detailed in Supplementary Data. Lists of genes with altered expression were independently analyzed with Ingenuity Pathways software[12] using a database of genetic and molecular interactions to identify networks of functionally related genes. Probability scores reflect the probability that genes are present in such networks by chance: a 1 in 100 chance is scored 2, 1 in 1,000 is scored 3, etc. The software assigns more weight to genes with higher fold expression changes. Genes whose expression showed the strongest association with EBV expression (correlation ≤−0.60) were used without such weighting.

[11] http://affymetrix.com.
[12] http://www.ingenuity.com.

Results

Gene expression in NPC and healthy nasopharyngeal epithelium is clearly distinct. Thirty-one NPC samples from 31 different cases and 10 normal reference samples were used for global human gene expression profiling. Of the normals, 6 were tumor-adjacent samples from NPC cases (including 4 matched with a tumor sample from the same patient) and 4 from patients who presented at the clinics but diagnosed NPC negative.

Comparison of genome-wide human gene expression profiles by unsupervised hierarchical clustering clearly distinguished normal epithelial samples from tumors (Fig. 1*A*), which was confirmed by multidimensional scaling, displaying the difference in summarized gene expression profiles between any two samples as their distance in a two-dimensional plane (Fig. 1*B*; ref. 17). Other class discovery techniques based on identifying signature gene sets also did not provide strong statistical support for NPC subclassification. Therefore, by global gene expression, NPCs are a relatively homogenous group sharing many features distinct from site- and patient-matched normals.

Eight hundred thirty-one probesets identify genes with significantly altered expression in NPC. A q-value/*t* test analysis (18) estimated that 49% of 54,675 human gene probesets measured altered expression between tumors and normals. Of these, 5,574 probesets detected altered expression at a 0.1% false discovery rate (FDR), a stringency imposed to limit the chance of erroneously reporting nondifferentially expressed genes to <1 in 1,000 (19). Independently, the EBarrays approach (15) found 6,123 probesets measuring differential expression at 0.1% FDR. These two lists overlap for 3,645 probesets, 3,439 of which (hereafter designated the shared list) measured an at least 1.5-fold change.
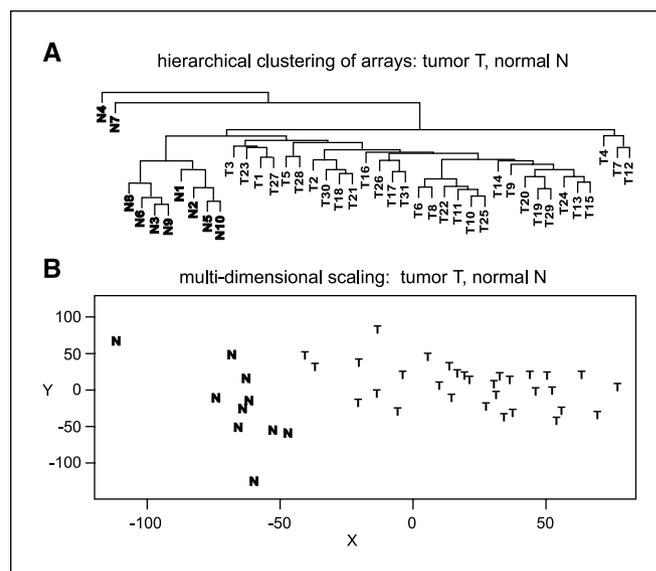

Figure 1. Pairwise comparison of whole human gene expression profiles across all samples distinguishes tumor from normal samples and shows that NPC tumors are a relatively homogeneous group sharing many distinguishing features. *A*, unsupervised hierarchical clustering according to the expression of all human genes. Length of vertical branches is a measure of the difference in summarized gene expression between samples. *B*, multidimensional scaling. In this two-dimensional projection, each sample is plotted onto an arbitrarily scaled XY plane such that the distance between any two samples best represents the total difference computed between their summarized complete gene expression profiles. *T*, tumor; *N*, normal.
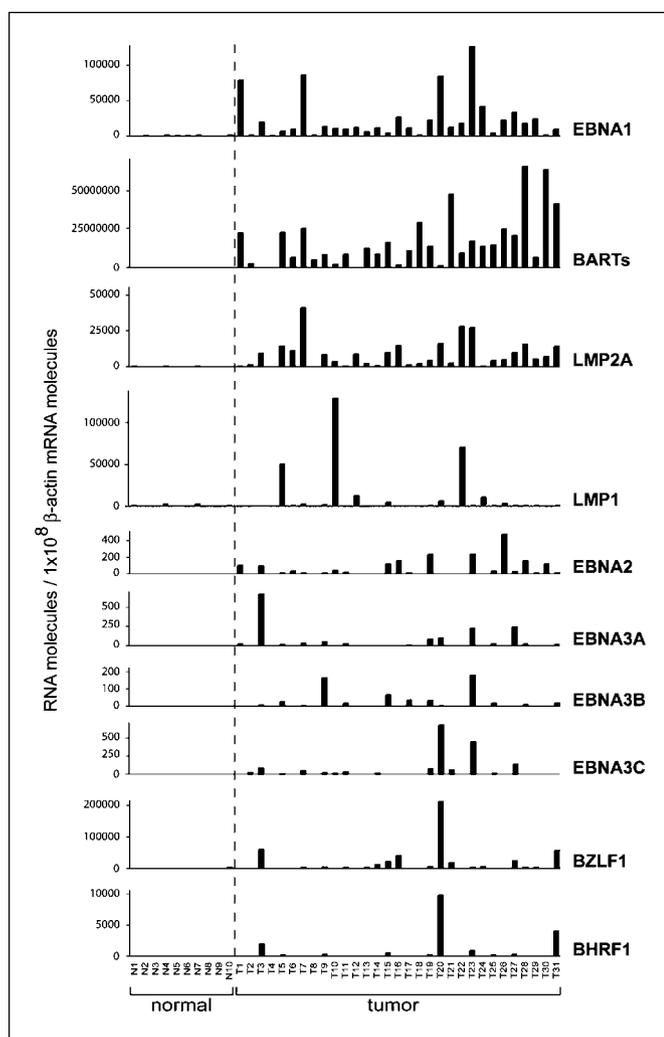
Figure 2. Real-time PCR-based measurements of EBV transcript levels normalized to β-actin mRNA levels show that tumors express varying levels of different EBV transcripts above background levels measured in normal samples. Note the varying Y-axes scales. Only EBNA1 and LMP2A mRNA and BART transcripts are consistently detected across all tumor samples (see also EBV gene expression data provided in Supplementary Table S6).

Analysis of donor-matched reference tissue minimizes the chance of inappropriately scoring genetic variability between patients as a difference between tumor and normal tissue. For the four matched sample pairs, 466 probesets measured consistent down-regulation and 581 probesets measured consistent up-regulation in the tumors (at least 1.5-fold). Of these, 429 and 402 probesets were on the shared list, respectively. Thus, two independent, stringent analyses identified 831 probesets that most consistently measured altered expression across the tumor collection and within the four matched tumor/normal pairs (gene IDs and information in Supplementary Table S3).

Many differentially expressed genes in NPC are involved in cell division and DNA replication. Gene ontology annotations describe gene products in terms of associated biological processes, cellular components, and molecular functions (16). More than 2,000 gene ontology categories of at least 10 probesets were examined for enrichment in genes represented by the 831 probesets. Thirty-six of 57 gene ontology classes enriched for up-regulated genes in the tumors described aspects of cell division and

DNA replication, and of 23 gene ontology classes enriched for down-regulated genes, 10 described cytoskeleton-associated processes, including 4, relating to microtubule-based movement (Supplementary Table S4).

The 831 probesets measuring differential expression in NPC were also analyzed using the Ingenuity Systems database,[12] which integrates published findings on biologically meaningful genetic or molecular gene/gene product interactions and identifies functionally related gene networks that overlap statistically significantly with a user-supplied gene list. Fourteen groups of genes were identified with a random chance probability of $\leq 10^{-6}$ (Supplementary Table S5). As in the gene ontology analysis, cell cycle and DNA replication/repair functions were prominent. Group 1, for example, contained 35 genes linked to cell cycle regulation, DNA replication and repair, or cell death. Of these, 23 were from the list of 831 probesets, a degree of overlap with a 10^{-25} chance probability (Supplementary Table S5).

Viral gene expression in NPC. NPC biology is the result of cellular and EBV gene expression. Therefore, in parallel with the microarray-based human gene expression analysis, we used quantitative real-time PCR to measure expression of all EBV latent genes (*EBNA1, EBNA2, EBNA3A, EBNA3B, EBNA3C, LMP1*, and *LMP2A*), two early lytic genes (*BZLF1* and *BHRF1*), and the EBV BART family of differentially spliced transcripts (20). All measurements were normalized to human β-actin mRNA levels.

No significant EBV gene expression was detected in healthy tissue (Fig. 2). In the tumors, EBNA1 and LMP2A RNAs and, particularly, BART RNAs were consistently detected, whereas LMP1 RNA was detectable in ~60% of cases (Fig. 2; Supplementary Table S6). Detection of EBNA1, LMP2A and LMP1, BARTs, and EBERs, as verified histochemically, is consistent with a type II EBV latency program in NPC (21). The levels of other viral latent transcripts (EBNA2 and EBNA3s) were 200- to 2,000-fold lower than those of EBNA1 and LMP2A (Supplementary Table S6), likely representing infiltrating lymphocytes commonly present in NPCs but representing <5% of cells in our microdissected samples. EBNA2 and EBNA3 signals did not arise from PCR contamination, as measurements between samples did not show coordinated variation in levels of the different EBV genes, and EBNA2 and EBNA3 signals were absent from normal tissue samples and negative controls included in the experimental setup. Detectable levels of BZLF1 and BHRF1 RNA were observed in a few tumors, possibly reflecting a subpopulation of cells undergoing lytic EBV replication (Fig. 2; Supplementary Table S6).

Viral and host gene expression are extensively inversely correlated. Because all NPCs are EBV positive, we tested for associations between EBV and human gene expression in NPC by identifying EBV dose-responsive effects. Tumors were ranked by expression of each individual viral and human gene, and correlations were calculated to identify human genes whose expression levels ranked the tumors most similarly or inversely to viral gene expression-based ranking. Thus, each viral gene had an association profile containing 54,675 host gene Spearman correlations. Figure 3C shows their empirical distribution for EBNA1. The association profiles for each of the EBV latent genes with host genes were generally quite similar as measured by Pearson correlation (Fig. 3A). Specifically, the LMP1 profile most closely resembled that of LMP2A. Similarly, EBNA3A, EBNA3B, and BHRF1 profiles were clustered. The EBNA3C association profile with human gene expression was only moderately similar to those of the other viral transcripts, whereas that of the BARTs was notably distinct.
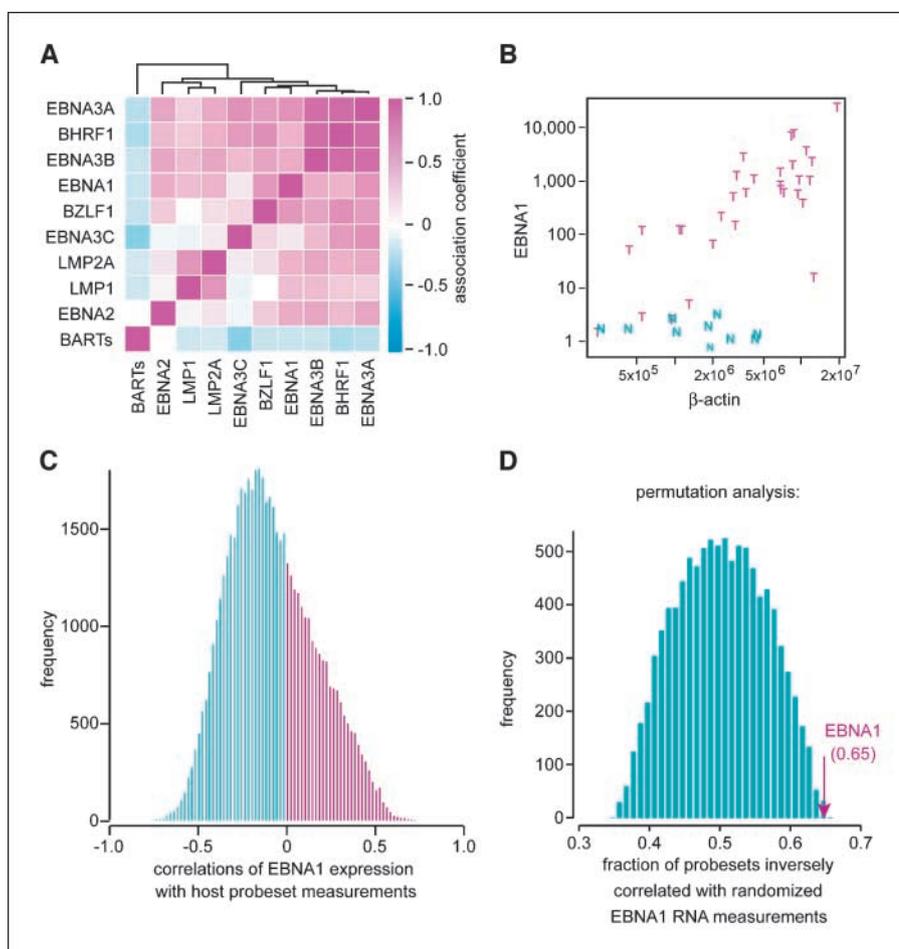
Figure 3. Increased EBV gene expression is dramatically associated with decreased expression levels of a large subset of human genes. *A,* correlation between the association profiles of viral genes. Each association profile measures the Spearman correlations between ranked measurements of the expression of a single viral gene and the full set of ranked host gene expression levels. *Colors,* levels of virus-host association according to the scale (*right*). *Top,* dendrogram clusters the viral genes accordingly. *B,* EBNA1 expression in the tumor and normal samples versus β-actin expression. *C,* frequencies of human probesets according to their positive (*red*) or negative (*blue*) correlation with EBNA1 expression. *D,* permutation analysis. Tumor labels were randomly shuffled with respect to measurements of EBNA1 RNA levels, and the fraction of host probesets, which was inversely correlated with EBNA1, was calculated. Distribution of the frequencies at which calculated fraction sizes occur when such permutation is repeated 10,000 times. *Red arrow,* true fraction of host probesets, which was inversely correlated with EBNA1 (0.65).

Of EBV RNAs whose expression correlated similarly with human gene expression (i.e., all except BART), EBNA1 RNA was consistently detected in all 31 tumors (Fig. 3*B*) and at higher levels than the others (Fig. 2; Supplementary Table S6). Therefore, EBNA1 RNA levels were the most reliable EBV expression variable for comparison to cellular gene profiles. Tumor ranking by EBNA1 RNA levels correlated strongly with those of a large subset (65%) of host mRNAs, indicated by a distribution that centered at approximately −0.2 rather than 0, which would be observed without association (Fig. 3*C*). Permutation analysis, randomizing EBNA1 RNA measurements among the tumors, showed that this level of inverse viral and human gene expression correlation occurs in <30 of 10,000 permutations (Fig. 3*D*).

Increased EBV gene expression is highly correlated with down-regulated expression of MHC class I antigen presentation genes. Of 2,354 gene ontology classes containing ≥10 probesets, only 3 were significantly enriched for genes whose reduced expression was correlated with increased EBV expression. All three of these classes, "antigen presentation and endogenous antigen," "MHC class I receptor activity," and "antigen processing and endogenous antigen via MHC class I," are functionally related. The average inverse correlation between gene expression in these three gene ontology classes and EBNA1 expression was unusually high (chance probability <10^{-9}). Figure 4 and Supplementary Table S7 illustrate the association between signals of EBNA1 and all 42 probesets representing 11 genes in one of these gene ontology classes, "antigen presentation and endogenous antigen." Most

notable in Fig. 4 is the inverse correlation between expression of EBNA1 and all MHC class I HLA genes as indicated by the decrease in HLA expression (shift from red to blue) from top to bottom as EBNA1 RNA levels increase. Similar inverse correlation, albeit more moderate, was observed for most other genes in this class, including *CD1D, HFE, HCG9,* and *TAP2* (Supplementary Table S7). HFE, expressed via ≥11 alternatively spliced transcripts, and CD1D encode MHC-like B2M-binding membrane proteins involved in iron absorption regulation and lipid antigen presentation, respectively (22, 23). TAP2 is a membrane-associated ATP-binding transporter protein with key roles in MHC class I–mediated antigen presentation (24). HCG9 lies within the MHC class I region but has no assigned function. Because all of these genes, except *CD1D*, are closely chromosomally linked, their EBV-associated inhibition might involve coordinated regulation at the DNA level.

Independently confirming the gene ontology analysis results, Ingenuity Pathway analysis of a group of 213 genes, whose reduced expression correlated most strongly with increased EBNA1 expression (Spearman rank correlation ≤ −0.6; Supplementary Table S8), identified three gene networks with a <10^{-11} chance probability (Table 1). The first group, with 12 focus genes among 35 functionally associated genes and an extremely low random chance probability of <10^{-16}, again contained several genes involved in MHC class I antigen presentation. The other two additional high-scoring groups of genes listed in Table 1 were involved in cancer-related functions, such as cell proliferation and DNA metabolism.

The inverse correlation of EBNA1 and HLA mRNA levels seemed similar to recently reported dose-responsive effects of two other herpesviruses on MHC class I HLA expression: HCMV and KSHV inhibited HLA expression by 2- to 3-fold and 2- to 5-fold, respectively (25–28). Similarly, in our study, quantitative real-time PCR showed that, compared with normal epithelium, the 10 highest EBNA1 NPC tumors had an average of 4.5-fold decreased HLA mRNA levels, whereas in the 10 lowest EBNA1 tumors HLA mRNA levels were decreased on average 2.1-fold (Supplementary Table S6).

LMP1-expressing tumors have increased antiapoptotic gene expression and decreased keratin gene expression. EBV latent protein LMP1 is an oncoprotein with antiapoptotic functions and associated with increased invasiveness and metastasis of EBV-associated tumors (29). Of the 31 tumor samples, 19 had detectable LMP1 mRNA levels. Using the EBarrays mixture approach (15) at 0.1% FDR, a set of 779 probesets measured up-regulated or down-regulated expression between LMP1-positive and LMP1-negative tumors (Supplementary Table S9). Among the 100 most highly up-regulated genes in LMP1-positive tumors were antiapoptotic *BCL2-related protein A1* (*BCL2A1*) and *Fas apoptotic inhibitory molecule* (*FAIM*). Other genes highly up-regulated in LMP1-positive tumors included *matrix metalloproteinase-1* (*MMP-1*), *Spi-B transcription factor* (*SPIB*), and *v-kit Hardy-Zuckerman 4 feline sarcoma viral oncogene homologue* (*KIT*). Among highly down-regulated genes were multiple keratins (*KRT4, KRT6B, KRT14, KRT23,* and *KRT24*).

Discussion

Our studies revealed that, on a global gene expression level, most aberrant gene expression in NPC concerns cell cycle regulation and cell division. However, levels of latent EBV gene expression in the same tumors showed extensive correlation with reduced expression of another large but different subset of human genes. In particular, viral expression, best represented by EBNA1 expression
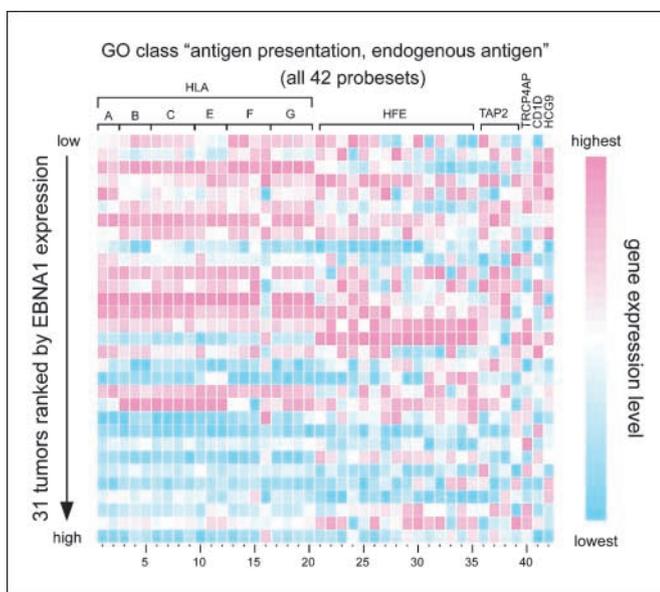

Figure 4. EBV gene expression is inversely correlated with the expression of genes involved in antigen presentation. Measurements for all 42 probesets in Gene Ontology (*GO*) class "antigen presentation and endogenous antigen." The tumors are ranked from top to bottom according to their EBNA1 expression levels. *Top,* gene names; *bottom,* numbers to further assist correlation with additional details in Supplementary Table S7.

levels, showed strong association with down-regulation of human genes involved in MHC class I–mediated antigen presentation.

Most aberrantly expressed genes reflect tumor proliferative state. Functional categorization of genes overexpressed and under-expressed in NPC was independently achieved by querying the gene ontology (16)[13] and Ingenuity Systems[12] databases, each including thousands of functional categories. Not unexpectedly, the majority of up-regulated genes related to the proliferative state of the tumors, including cell division and DNA replication, recombination, and repair. Overexpressed genes included *BUB1B* and *MAD2L1*, mitotic spindle assembly checkpoint components responsible for proper chromosome segregation (30, 31). Their aberrant expression could be associated with chromosomal alterations frequently observed in NPC (32). Cyclin E2, whose expression peaks at the G_1-S phase, is overexpressed in NPC as in many tumor-derived cell lines (33). Also up-regulated was *NBS1*, involved in DNA double-strand break repair and DNA damage-induced checkpoint activation (34).

Recently, a smaller study profiling expression of ~9,000 genes in eight laser-microdissected NPC tissue samples reported 154 differentially expressed genes (12). Of those, only 7 up-regulated and 19 down-regulated genes were in our core set of 831 highly validated, differentially expressed genes (Supplementary Table S3). This limited overlap likely reflects a different choice of reference samples, as the previous study compared NPC RNA with pooled RNA from cell lines of various origins (including nonepithelial origins) rather than with normal healthy nasopharyngeal epithelium. Among genes that both studies measured as overexpressed in tumors were *mitosin* and *Topoisomerase IIα*, which are essential for proper chromosome segregation (35, 36), *MUC1*, which is overexpressed in many carcinomas and related to invasiveness and poor prognosis (37, 38), and G_2-M checkpoint gene *CHEK1*, up-regulated in response to DNA damage (39). CHEK1 inhibitors abrogating the G_2 block enhance radiation toxicity in human lymphoma and colon cancer cell lines (40). Because radiotherapy is the recommended treatment for NPC, sensitizing tumor cells to radiation with CHEK1 inhibitors might improve outcome.

EBV is highly associated with modulation of antigen presentation in NPC. The quantitative real-time PCR data agree with previous assessment of NPC as displaying a type II EBV latency program. As in other EBV-associated epithelial malignancies, *EBNA1* is the single viral gene product that is invariably detected, whereas a subset of tumors is positive for *LMP1, LMP2A,* or other viral oncogenes (41). In addition, a family of differentially spliced viral transcripts, the BART RNAs, is highly expressed in NPC (42, 43). Most EBV transcripts were undetectable in micro-array-based assays using 24-mer or 70-mer oligonucleotide platforms (data not shown), which underscores the importance of low-abundance transcripts that remain undetected by microarrays.

With the noted exception of BART transcripts, expression levels of EBV genes in NPC were similarly and inversely correlated with the expression of a large subset of human genes (Fig. 3*A*; Supplementary Table S8). Therefore, the changes in host gene expression were not necessarily attributable to any particular single viral gene product. For further comparisons with human gene expression, we chose EBNA1 to represent EBV gene expression because, among viral genes sharing correlated expression with host gene expression, EBNA1 was consistently detected in all tumor samples, in line with its essential role in faithful segregation of EBV

---

[13] http://www.geneontology.org/.

Table 1. Functional gene networks containing multiple human genes whose down-regulated expression strongly correlates with increased EBV expression

Group	Global functions of genes in this group	Probability score*	Genes present in this group
1	Cell-to-cell signaling and interaction. Cellular growth and proliferation. Immune and lymphatic system. Development and function.	10^{-16}	*APS, B2M, BAT9, CANX, CD3D,* **CD3Z, CISH, CTLA4,** *DNM1, FACL2, GRB2,* **GRF2,** *H2-LD,* **HLA-A,** *HLA-B,* **HLA-F** [†]*, IRS1, JAK2,* **KCNAB2,** *LILRB1, LILRB2, LY6A, NISCH, OSI,* **PACSIN1,** *PCYT1A, PRKCZ,* **PTPN1,** *PTPRA,* **PTPRE, RPS6KA1,** *SH2B, SP1,* **SREBF1,** *TAP2*
2	Cancer. Cellular growth and proliferation. Cellular development.	10^{-14}	*CD36, CDKN1C, CDKN2A,* ***CRX,*** *FYN,* **GATA2,** *HMGB1, IL6, ILK,* **ITGB3,** *ITGB5,* **LDB1, LIMS2,** *LMO1, LMO2, NEUROD1,* **NHLH1,** *PARVA,* **PITX1, PPARD** [†]*, PPP1CC,* **PPP1R9B, PRRX1,** *PSMD10, PSMD12,* **PSMD5,** *PSMD7, PSMD8, PSMD9, RB1, SA-BETA-GAL, TAL1, TCF3, TWIST1,* **VAV2**
3	Cell death. Cell cycle. DNA replication, recombination, and repair.	10^{-11}	*APEX1, CBX3, CBX5, CDC25C, CDC42, CHEK2,* **CSF2, CYFIP2,** *DAG1, DHX9, DNMT1, FMR1, FXR1, FXR2, GADD45A,* **GADD45B,** *IFI16,* **LENEP,** *MAP3K4, MAP4,* **MCF2L,** *MSH2, MYC, NSEP1, PAK2, PCNA,* **PLK3, PRX,** *PURA, RPS7, RUVBL2,* **SP100,** *WRN, YAF2,* **ZNF151**

NOTE: Genes in bold italics are among 213 genes (focus genes) whose reduced expression strongly correlates with increased EBV gene expression (Spearman correlation ≤−0.6) and were used as input for the analysis.
*Random chance of the genes in bold italics being found together in a single network.
[†]Detected from multiple probesets.

DNA with host chromosomes during mitosis (44). We did not use BART transcripts to represent overall viral gene expression because differences in BART transcript levels surprisingly did not correlate with any expression changes in either EBV or host genes. The high levels of BART expression, approaching β-actin mRNA levels, may be saturating so that dose responsiveness of host genes to the actions of BART is no longer evident. In addition, our quantitative real-time PCR analysis did not distinguish between differentially spliced BART transcripts encoding BARF0, A73, RPMS1, and RPMS1A (42). RPMS1 binds CBF1, a mediator of Notch signaling, possibly negatively regulating Notch signal transduction (42). A73 has been suggested to contribute to tumor cell development via its association with RACK1 (42). The high abundance of BART RNAs suggests important function(s) in NPC that needs further study.

Gene ontology analysis showed that, for host genes with highly EBV-associated decreases in expression, significantly enriched annotations were antigen processing, presentation, and receptor activity. Most strongly inverse correlated with EBNA1 expression were the expression levels of all MHC class I HLA genes (Fig. 4), which play central roles in immunity by presenting foreign peptides to cytotoxic T cells. Ingenuity Pathway analysis independently identified HLA-A and HLA-F in the highest scoring functional gene network. The strong correlation between EBV gene expression and down-regulation of HLA expression is particularly intriguing in light of other links between MHC class I HLAs, NPC, and EBV. Recent high-resolution HLA typing confirmed a particular HLA allele common in individuals of Chinese, but not Caucasian, descent as a NPC risk factor (5). This HLA allele might be associated with greater susceptibility to suppression by EBV, reduced efficiency for presenting EBV or host antigens, or both.

Because histopathology and quantitative real-time PCR showed that EBV is present in all NPC tumor cells but at varying genome copy numbers and/or expression levels, the strong inverse correlation in NPC between HLA and EBV gene expression (Fig. 4) implies dose responsiveness similar to down-regulation of MHC class I surface expression by other herpesviruses (25–28). Overall, our results are consistent with reports that NPC cells and cultured NPC

cell lines display class I cell surface HLA (45, 46) but indicate that they do so at reduced levels. These findings imply that, in NPCs, EBV inhibits MHC class I presentation of its own antigens, including TAP-independent presentation of LMP2A (47), and presentation of other antigens, facilitating tumor cell evasion of immunosurveillance. This would increase tumor cell survival while allowing elevated viral gene expression and consequently enhanced tumorigenic potential through viral functions, such as from LMP1. The observation that tissue-cultured NPC cells rapidly lose EBV is also consistent with an immunosurveillance-based selection mechanism.

Other genes whose expression is inversely correlated with EBNA1 expression. Expression of PSMD5, part of the 19S regulator of the 26S proteasome, showed the strongest inhibition with increasing levels of EBNA1, suggesting a function for EBV in down-regulating protein turnover. This would be separate from generating antigenic peptides presented by MHC class I, which is the responsibility of a modified proteasome with the 11S regulator instead of 19S (48). EBNA1 RNA levels were used only to represent overall viral gene expression, and PSMD5 regulation does not necessarily relate to previous suggestions that Gly-Ala repeat sequences in EBNA1 prevent its proteosomal degradation (49, 50).

In B cells, EBNA1 inhibits apoptosis, a potential advantage for EBV-positive tumor cells (51). Latent EBV infection protects Burkitt lymphoma–derived cells from cell cycle arrest and apoptosis by interfering with a G_2 phase or mitotic checkpoint, possibly through EBNA1, the EBNA3 family of proteins (EBNA3A, EBNA3B, and EBNA3C), the EBERs, or the BARTs (52). Not inconsistently, our findings in epithelial cells show that EBNA1 expression correlates with down-regulated expression of AKIP, SCYL1, and NIN (Supplementary Table S8), all associated with cell cycle checkpoints. AKIP down-regulates and interacts specifically with Aurora-A kinase, whose overexpression transforms cultured cells and causes aneuploidy via aberrant chromosomal segregation (53). SCYL1 is a centrosome-associated, cell cycle–related protein whose dysfunction likely plays a role in cancer (54). NIN encodes a centrosomal protein important for positioning and anchoring microtubule minus ends in epithelial cells and correct chromosomal segregation (55).

By suppressing accumulation of these mRNAs, EBNA1 might contribute toward bypassing the mitotic spindle checkpoint and eventual chromosomal disarray in tumor cells.

Antiapoptotic and metastasis-associated genes are highly overexpressed in LMP1-positive tumors. EBV LMP1 is a well-studied oncogene (41). Accordingly, we identified human genes differentially expressed between tumors with or without detectable LMP1 expression (Supplementary Table S9). Many keratin genes were down-regulated in LMP1-expressing tumors, including *Keratin 4*, which is expressed in differentiated epithelia (56), perhaps reflecting the contribution of LMP1 to the undifferentiated state of NPCs. Independently validating our results is the overexpression of tyrosine kinase KIT in LMP1-expressing tumors (Supplementary Table S9) as previously observed in EBV-positive, undifferentiated nonkeratinizing NPCs (57). Recently, KIT was shown to be a major component in KSHV-induced cell transformation (58).

Also up-regulated in LMP1-positive tumors are antiapoptotic genes, such as *FAIM* (59) and *BCL2A1*, which blocks caspase activation by reducing mitochondrial cytochrome *c* release (60). LMP1 inhibits apoptosis in Burkitt's lymphoma by up-regulating BCL2A1 transcription through interactions with tumor necrosis factor receptor/CD40 signaling (61, 62).

LMP1-positive tumors had 2.5-fold increased levels of MMP-1 expression (Supplementary Table S9), in keeping with a recent targeted study of MMP-1 in NPCs (63). MMP-1 and other MMPs facilitate extracellular matrix breakdown and are associated with metastasis and poor prognosis. High MMP-1 expression might contribute to the highly malignant nature of NPC. LMP1-positive tumors also overexpressed SPIB, consistent with epithelial cell studies showing that LMP1 induces MMP-1 transcription via ETS transcription factors, such as SPIB (64). In addition, another recent report described a possible link between EBV LMP2A and NPC metastasis (65).

References

1. Parkin DM, Bray F, Ferlay J, Pisani P. Global cancer statistics, 2002. CA Cancer J Clin 2005;55:74–108.
2. Chan JKC, Bray F, McCarron P, et al. Nasopharyngeal carcinoma. In: Barnes L, Eveson JW, Reichart P, Sidransky D, editors. Pathology and genetics of head and neck tumors. Lyon: IARC Press; 2005. p. 85–97.
3. Chan SH, Day NE, Kunaratnam N, Chia KB, Simons MJ. HLA and nasopharyngeal carcinoma in Chinese—a further study. Int J Cancer 1983;32:171–6.
4. Lu SJ, Day NE, Degos L, et al. Linkage of a nasopharyngeal carcinoma susceptibility locus to the HLA region. Nature 1990;346:470–1.
5. Hildesheim A, Apple RJ, Chen CJ, et al. Association of HLA class I and II alleles and extended haplotypes with nasopharyngeal carcinoma in Taiwan. J Natl Cancer Inst 2002;94:1780–9.
6. Ward MH, Pan WH, Cheng YJ, et al. Dietary exposure to nitrite and nitrosamines and risk of nasopharyngeal carcinoma in Taiwan. Int J Cancer 2000;86:603–9.
7. Hildesheim A, Anderson LM, Chen CJ, et al. CYP2E1 genetic polymorphisms and risk of nasopharyngeal carcinoma in Taiwan. J Natl Cancer Inst 1997;89:1207–12.
8. Kongruttanachok N, Sukdikul S, Setavarin S, et al. Cytochrome *P450* 2E1 polymorphism and nasopharyngeal carcinoma development in Thailand: a correlative study. BMC Cancer 2001;1:4.
9. Cho EY, Hildesheim A, Chen CJ, et al. Nasopharyngeal carcinoma and genetic polymorphisms of DNA repair enzymes XRCC1 and hOGG1. Cancer Epidemiol Biomarkers Prev 2003;12:1100–4.
10. Fung LF, Lo AK, Yuen PW, Liu Y, Wang XH, Tsao SW. Differential gene expression in nasopharyngeal carcinoma cells. Life Sci 2000;67:923–36.
11. Xie L, Xu L, He Z, et al. Identification of differentially expressed genes in nasopharyngeal carcinoma by means of the Atlas human cancer cDNA expression array. J Cancer Res Clin Oncol 2000;126:400–6.
12. Sriuranpong V, Mutirangura A, Gillespie JW, et al. Global gene expression profile of nasopharyngeal carcinoma by laser capture microdissection and complementary DNA microarrays. Clin Cancer Res 2004;10:4944–58.
13. Dumur CI, Garrett CT, Archer KJ, Nasim S, Wilkinson DS, Ferreira-Gonzalez A. Evaluation of a linear amplification method for small samples used on high-density oligonucleotide microarray analysis. Anal Biochem 2004;331:314–21.
14. Irizarry RA, Hobbs B, Collin F, et al. Exploration, normalization, and summaries of high density oligonucleotide array probe level data. Biostatistics 2003;4:249–64.
15. Kendziorski CM, Newton MA, Lan H, Gould MN. On parametric empirical Bayes methods for comparing multiple groups using replicated gene expression profiles. Stat Med 2003;22:3899–914.
16. Ashburner M, Ball CA, Blake JA, et al. Gene ontology: tool for the unification of biology. The Gene Ontology Consortium. Nat Genet 2000;25:25–9.
17. Khan J, Simon R, Bittner M, et al. Gene expression profiling of alveolar rhabdomyosarcoma with cDNA microarrays. Cancer Res 1998;58:5009–13.
18. Storey JD, Tibshirani R. Statistical significance for genomewide studies. Proc Natl Acad Sci U S A 2003;100:9440–5.
19. Benjamini Y, Hochberg Y. Controlling the false discovery rate: a practical and powerful approach to multiple testing. J R Stat Soc B 1995;57:289–300.
20. Kieff E, Rickinson A. Epstein-Barr virus and its replication. 4th ed. Philadelphia: Lippincott Williams and Wilkins; 2001.
21. Lopes V, Young LS, Murray PG. Epstein-Barr virus-associated cancers: aetiology and treatment. Herpes 2003;10:78–82.
22. Kawano T, Cui J, Koezuka Y, et al. CD1d-restricted and TCR-mediated activation of vα14 NKT cells by glycosylceramides. Science 1997;278:1626–9.
23. Roy CN, Penny DM, Feder JN, Enns CA. The hereditary hemochromatosis protein, HFE, specifically regulates transferrin-mediated iron uptake in HeLa cells. J Biol Chem 1999;274:9022–8.
24. van Endert PM, Saveanu L, Hewitt EW, Lehner P. Powering the peptide pump: TAP crosstalk with energetic nucleotides. Trends Biochem Sci 2002;27:454–61.
25. Benz C, Reusch U, Muranyi W, Brune W, Atalay R, Hengel H. Efficient downregulation of major histocompatibility complex class I molecules in human epithelial cells infected with cytomegalovirus. J Gen Virol 2001;82:2061–70.
26. Trgovcich J, Cebulla C, Zimmerman P, Sedmak DD. Human cytomegalovirus protein pp71 disrupts major histocompatibility complex class I cell surface expression. J Virol 2006;80:951–63.
27. Tomescu C, Law WK, Kedes DH. Surface down-regulation of major histocompatibility complex class I, PE-CAM, and ICAM-1 following *de novo* infection of endothelial cells with Kaposi's sarcoma-associated herpesvirus. J Virol 2003;77:9669–84.
28. Ishido S, Wang C, Lee BS, Cohen GB, Jung JU. Downregulation of major histocompatibility complex class I molecules by Kaposi's sarcoma-associated herpesvirus K3 and K5 proteins. J Virol 2000;74:5300–9.
29. Lo AK, Liu Y, Wang XH, et al. Alterations of biologic properties and gene expression in nasopharyngeal epithelial cells by the Epstein-Barr virus-encoded latent membrane protein 1. Lab Invest 2003;83:697–709.
30. Lampson MA, Kapoor TM. The human mitotic checkpoint protein BubR1 regulates chromosome-spindle attachments. Nat Cell Biol 2005;7:93–8.
31. Li Y, Benezra R. Identification of a human mitotic checkpoint gene: hsMAD2. Science 1996;274:246–8.
32. Hui AB, Lo KW, Leung SF, et al. Detection of recurrent chromosomal gains and losses in primary nasopharyngeal carcinoma by comparative genomic hybridisation. Int J Cancer 1999;82:498–503.
33. Gudas JM, Payton M, Thukral S, et al. Cyclin E2, a novel G_1 cyclin that binds Cdk2 and is aberrantly expressed in human cancers. Mol Cell Biol 1999;19:612–22.
34. Varon R, Vissinga C, Platzer M, et al. Nibrin, a novel DNA double-strand break repair protein, is mutated in Nijmegen breakage syndrome. Cell 1998;93:467–76.
35. Carpenter AJ, Porter AC. Construction, characterization, and complementation of a conditional-lethal DNA topoisomerase IIα mutant human cell line. Mol Biol Cell 2004;15:5700–11.
36. Yang Z, Guo J, Chen Q, Ding C, Du J, Zhu X. Silencing mitosin induces misaligned chromosomes, premature chromosome decondensation before anaphase onset, and mitotic cell death. Mol Cell Biol 2005;25:4062–74.
37. Alos L, Lujan B, Castillo M, et al. Expression of membrane-bound mucins (MUC1 and MUC4) and secreted mucins (MUC2, MUC5AC, MUC5B, MUC6, and MUC7) in mucoepidermoid carcinomas of salivary glands. Am J Surg Pathol 2005;29:806–13.

38. Baldus SE, Monig SP, Huxel S, et al. MUC1 and nuclear β-catenin are coexpressed at the invasion front of colorectal carcinomas and are both correlated with tumor prognosis. Clin Cancer Res 2004;10:2790–6.

39. Sanchez Y, Wong C, Thoma RS, et al. Conservation of the Chk1 checkpoint pathway in mammals: linkage of DNA damage to Cdk regulation through Cdc25. Science 1997;277:1497–501.

40. Xiao HH, Makeyev Y, Butler J, Vikram B, Franklin WA. 7-Hydroxystaurosporine (UCN-01) preferentially sensitizes cells with a disrupted TP53 to γ radiation in lung cancer cell lines. Radiat Res 2002;158:84–93.

41. Raab-Traub N. Epstein-Barr virus in the pathogenesis of NPC. Semin Cancer Biol 2002;12:431–41.

42. Smith PR, de Jesus O, Turner D, et al. Structure and coding content of CST (BART) family RNAs of Epstein-Barr virus. J Virol 2000;74:3082–92.

43. Chen HL, Lung MM, Sham JS, Choy DT, Griffin BE, Ng MH. Transcription of BamHI-A region of the EBV genome in NPC tissues and B cells. Virology 1992;191:193–201.

44. Hammerschmidt W, Sugden B. Epstein-Barr virus sustains Burkitt's lymphomas and Hodgkin's disease. Trends Mol Med 2004;10:331–6.

45. Khanna R, Busson P, Burrows SR, et al. Molecular characterization of antigen-processing function in nasopharyngeal carcinoma (NPC): evidence for efficient presentation of Epstein-Barr virus cytotoxic T-cell epitopes by NPC cells. Cancer Res 1998;58:310–4.

46. Lee SP, Chan AT, Cheung ST, et al. CTL control of EBV in nasopharyngeal carcinoma (NPC): EBV-specific CTL responses in the blood and tumors of NPC patients and the antigen-processing function of the tumor cells. J Immunol 2000;165:573–82.

47. Khanna R, Burrows SR, Moss DJ, Silins SL. Peptide transporter (TAP-1 and TAP-2)-independent endogenous processing of Epstein-Barr virus (EBV) latent membrane protein 2A: implications for cytotoxic T-lymphocyte control of EBV-associated malignancies. J Virol 1996;70:5357–62.

48. Coux O, Tanaka K, Goldberg AL. Structure and functions of the 20S and 26S proteasomes. Annu Rev Biochem 1996;65:801–47.

49. Levitskaya J, Sharipo A, Leonchiks A, Ciechanover A, Masucci MG. Inhibition of ubiquitin/proteasome-dependent protein degradation by the Gly-Ala repeat domain of the Epstein-Barr virus nuclear antigen 1. Proc Natl Acad Sci U S A 1997;94:12616–21.

50. Blake N, Lee S, Redchenko I, et al. Human CD8$^+$ T cell responses to EBV EBNA1: HLA class I presentation of the (Gly-Ala)-containing protein requires exogenous processing. Immunity 1997;7:791–802.

51. Kennedy G, Komano J, Sugden B. Epstein-Barr virus provides a survival factor to Burkitt's lymphomas. Proc Natl Acad Sci U S A 2003;100:14269–74.

52. Wade M, Allday MJ. Epstein-Barr virus suppresses a G(2)/M checkpoint activated by genotoxins. Mol Cell Biol 2000;20:1344–60.

53. Kiat LS, Hui KM, Gopalan G. Aurora-A kinase interacting protein (AIP), a novel negative regulator of human Aurora-A kinase. J Biol Chem 2002;277:45558–65.

54. Kato M, Yano K, Morotomi-Yano K, Saito H, Miki Y. Identification and characterization of the human protein kinase-like gene NTKL: mitosis-specific centrosomal localization of an alternatively spliced isoform. Genomics 2002;79:760–7.

55. Chen CH, Howng SL, Cheng TS, Chou MH, Huang CY, Hong YR. Molecular characterization of human ninein protein: two distinct subdomains required for centrosomal targeting and regulating signals in cell cycle. Biochem Biophys Res Commun 2003;308:975–83.

56. Luo A, Kong J, Hu G, et al. Discovery of Ca^{2+}-relevant and differentiation-associated genes downregulated in esophageal squamous cell carcinoma using cDNA microarray. Oncogene 2004;23:1291–9.

57. Bar-Sela G, Kuten A, Ben-Eliezer S, Gov-Ari E, Ben-Izhak O. Expression of HER2 and C-KIT in nasopharyngeal carcinoma: implications for a new therapeutic approach. Mod Pathol 2003;16:1035–40.

58. Moses AV, Jarvis MA, Raggo C, et al. Kaposi's sarcoma-associated herpesvirus-induced upregulation of the c-kit proto-oncogene, as identified by gene expression profiling, is essential for the transformation of endothelial cells. J Virol 2002;76:8383–99.

59. Schneider TJ, Fischer GM, Donohoe TJ, Colarusso TP, Rothstein TL. A novel gene coding for a Fas apoptosis inhibitory molecule (FAIM) isolated from inducibly Fas-resistant B lymphocytes. J Exp Med 1999;189:949–56.

60. Wang CY, Guttridge DC, Mayo MW, Baldwin AS, Jr. NF-κB induces expression of the Bcl-2 homologue A1/Bfl-1 to preferentially suppress chemotherapy-induced apoptosis. Mol Cell Biol 1999;19:5923–9.

61. D'Souza B, Rowe M, Walls D. The bfl-1 gene is transcriptionally upregulated by the Epstein-Barr virus LMP1, and its expression promotes the survival of a Burkitt's lymphoma cell line. J Virol 2000;74:6652–8.

62. D'Souza BN, Edelstein LC, Pegman PM, et al. Nuclear factor κB-dependent activation of the antiapoptotic bfl-1 gene by the Epstein-Barr virus latent membrane protein 1 and activated CD40 receptor. J Virol 2004;78:1800–16.

63. Lu J, Chua HH, Chen SY, Chen JY, Tsai CH. Regulation of matrix metalloproteinase-1 by Epstein-Barr virus proteins. Cancer Res 2003;63:256–62.

64. Kondo S, Wakisaka N, Schell MJ, et al. Epstein-Barr virus latent membrane protein 1 induces the matrix metalloproteinase-1 promoter via an Ets binding site formed by a single nucleotide polymorphism: enhanced susceptibility to nasopharyngeal carcinoma. Int J Cancer 2005;115:368–76.

65. Pegtel DM, Subramanian A, Sheen T-S, Tsai C-H, Golub TR, Thorley-Lawson DA. Epstein-Barr virus-encoded LMP2A induces primary epithelial cell migration and invasion: possible role in nasopharyngeal carcinoma metastasis. J Virol 2005;79:15430–42.